

Resonant Activation Phenomenon for Non-Markovian Potential-Fluctuation Processes

Tomáš Novotný*

Institute of Physics, Academy of Sciences of the Czech Republic, Na Slovance 2, 182 21 Prague, Czech Republic

Petr Chvosta†

Department of Macromolecular Physics, Faculty of Mathematics and Physics,

Charles University, V Holešovičkách 2, 180 00 Prague, Czech Republic

(Dated: February 5, 2020)

We consider a generalization of the model by Doering and Gadoua [Phys. Rev. Lett. **69**, 2318 (1992)] to non-Markovian potential-switching generated by arbitrary renewal processes. For the Markovian switching process, we recover the original results of Doering and Gadoua for the mean first passage time and we extend these results by giving a complete description of the absorption process. For all non-Markovian processes having the first two moments of the waiting time distributions, we get qualitatively the same results as in the Markovian case. However, for distributions without the second or even the first moment, the mean first passage time curves do not exhibit the resonant activation minimum. We thus come to the conjecture that the generic mechanism of the resonant activation fails for fluctuating processes widely deviating from Markovian.

I. INTRODUCTION

The dynamical behaviour of an overdamped Brownian particle acted upon by the Gaussian white noise thermal force is a well understood classical problem [1, 2, 3]. This is also true if the problem incorporates various types of boundaries and/or if we wish to characterize the (random) time to reach a definite region from a given starting position. In the last decade, however, the diffusion dynamics has been reexamined in systems in which other simultaneous and independent dynamical mechanisms are present. The new achievements have substantially broadened the field—consult Refs. [4, 5] for the recent reviews and the references.

Imagine a diffusing particle acted upon by an additional time-dependent force. The additional influence can be either *deterministic* (e.g. an external time-periodic driving) or *stochastic* (e.g. an intrinsic random modulation of the potential profile). Up to now, these two subproblems have been analyzed separately by using specific and different operational procedures. Clearly, by changing the statistical properties of the additional force, both cases can be interconnected. One motivation of the present paper consists in examination of a method which works in both the deterministic and the stochastic case.

We select a problem modest in its complexity. Namely, our calculation is based on the “archetypal” Doering-Gadoua model [6, 7] of the one dimensional diffusion in a linear potential with a stochastically changing slope. The motion is restricted to a finite interval (called the “safe domain” in the following) by introducing a reflecting wall at the right end of the safe domain and by placing a trap at the left end. The potential-switching is controlled by a symmetric stationary dichotomous noise. Doering and Gadoua have taken the Markovian variant of this noise with a given switching rate.

Once we introduce the absorbing boundary, the composite dynamics is intimately connected with the capturing effects. At the same time, the dynamics strongly depends on the mean potential-switching frequency. First, assume a very slow switching rate. Then the motion is simply the average of two oppositely biased diffusive motions. In the other limit, for a very fast switching, the particle cannot follow the changes of the potential profile and it moves in an average effective potential. In the case of the above mentioned *symmetric* modulation, this effective potential is zero and the particle is driven exclusively by the original thermal noise. Its intensity (i.e. the corresponding temperature) controls the escape time. Next, imagine we start with this infinitely fast switching case and gradually decrease the switching rate. Then the switching process effectively behaves as a weak white noise with its intensity being inversely proportional to the potential-switching rate. This additional white noise is added to the original thermal one and the sum of both noises can be mimicked by a single Gaussian white noise with an enhanced intensity (i.e. an increased temperature). As a result, the capturing process is accelerated. This results in the Resonant Activation

*novotnyt@fzu.cz; <http://www.fzu.cz/~novotnyt>

†chvosta@kmf.troja.mff.cuni.cz

(RA) phenomenon [4]. Differently speaking, there exists a specific value of the switching frequency which optimizes the capturing process. The RA phenomenon has attracted a wide attention and it has been intensively discussed in the last years [4, 7].

A quantitative analysis of the RA effects represents another central point of the present work. Specifically, we want to analyze the stability of the RA phenomenon against variations of the random point process which governs properties of the dichotomous potential force. From an operational point of view, we have to bypass the standard (semigroup like) procedures which rest on the Markovian nature of the potential fluctuations. Rather, our method resembles the one used in the context of the coherent stochastic resonance [8, 9]. Specifically, we employ the method developed in Ref. [10], which we have found to be especially well suited to a quantitative analysis of such problems.

Implementing our method, we can directly investigate the most interesting quantities describing the composite dynamics. Namely, we study the weight of the trajectories captured by the absorbing boundary while the potential has resided in a specific state. To this end, we introduced the device of *two channel* absorption boundary, a given channel gathering the trajectories which arrive at the boundary while the potential stays in a given state. This formulation allows for a complete time resolved characterization of the channel filling process. Nevertheless, in our calculations, we focused on just two quantities. In particular, we calculate switching rate dependencies of the Asymptotic Boundary Channel Occupation (ABCO) and the Mean First Passage Time (MFPT).

The paper is organized as follows. In Sec. II, we present details of the model setting. In Sec. III, we develop our main general results. We construct the switching averaged and the state-of-potential resolved probability density for the particle position and we give explicit formulae for ABCO and MFPT. These results are general in the sense that they are valid for any statistics of the underlying potential-switching point process. We elaborate on these results in Sec. IV which has been divided in two parts. First, we give the complete explicit solution to the Markovian-switching case, including the channel resolved formulae describing the capturing process. The second part presents calculations in the non-Markovian cases. Here, by examining several specific examples of the switching-process statistics, we acquire an explicit description of the quantities introduced above, ABCO and MFPT. Conclusions are drawn in the last section and some mathematical details of the numerical procedures in Sec. IV B are given in the Appendix ??.

II. MODEL

Assume that the overdamped Brownian particle is driven by two forces: the Gaussian white noise unbiased thermal force $\tilde{G}(\tilde{t})$ (let $k_B T/\eta$ be the corresponding diffusion constant, i.e. $2\eta k_B T \delta(\tilde{t} - \tilde{t}')$ is the autocorrelation function of the thermal force), and the homogeneous force $\tilde{F} Q(\tilde{t})$, $\tilde{F} \geq 0$, which derives from the linear potential with a slope randomly switched between two values $\pm \tilde{F}$. The normalized symmetric dichotomous noise $Q(\tilde{t})$ exhibits jumps between two values ± 1 at random times. Statistical properties of the underlying random point process will be detailed below.

The emerging dynamics is controlled by the viscous Langevin equation

$$\eta \frac{d}{d\tilde{t}} \tilde{X}(\tilde{t}) = \tilde{F} Q(\tilde{t}) + \tilde{G}(\tilde{t}) . \quad (1)$$

Our main objective is the analysis of this equation in connection with a specific arrangement of boundaries: the one dimensional diffusive motion is restricted onto a given interval (the safe domain) by introducing the *reflecting* boundary at $L > 0$ and the *absorbing* boundary at the origin. The problems involving an absorption state are intimately related to the statistics of the first passage events.

In order to get a feel for the composite dynamics, assume for the moment that the potential is frozen in one of its two possible slopes (in all formulae below, the upper (lower) sign refers to the positive (negative) potential force and the upper index ‘⁽⁰⁾’ designates the fixed potential quantities). Hence the dynamics is a simple Brownian motion of an overdamped particle in a linear potential with the above mentioned boundary conditions. The Fokker-Planck equations for the corresponding Green’s functions read

$$\frac{\partial}{\partial \tilde{t}} \tilde{G}_{\pm}^{(0)}(\tilde{x}, \tilde{y}; \tilde{t}) = -\frac{\partial}{\partial \tilde{x}} \left[-\frac{k_B T}{\eta} \frac{\partial}{\partial \tilde{x}} \tilde{G}_{\pm}^{(0)}(\tilde{x}, \tilde{y}; \tilde{t}) \pm \frac{\tilde{F}}{\eta} \tilde{G}_{\pm}^{(0)}(\tilde{x}, \tilde{y}; \tilde{t}) \right] . \quad (2)$$

The bracketed expression on the right hand side represents the probability current $\tilde{J}_{\pm}^{(0)}(\tilde{x}, \tilde{y}; \tilde{t})$. We assume the initial condition $\tilde{G}_{\pm}^{(0)}(\tilde{x}, \tilde{y}; 0) = \delta(\tilde{x} - \tilde{y})$, where $\tilde{y} \in (0, L)$. The above mentioned boundary conditions imply the requirements $\tilde{J}_{\pm}^{(0)}(L, \tilde{y}; \tilde{t}) = 0$ and $\tilde{G}_{\pm}^{(0)}(0, \tilde{y}; \tilde{t}) = 0$.

Now, we introduce dimensionless variables. The potential force is represented by the parameter $F = \tilde{F}L/(k_B T)$, the dimensionless coordinate is $x = \tilde{x}/L$, and the dimensionless time reads $t = \tilde{t}k_B T/(\eta L^2)$. We thus get from Eq.

(2)

$$\frac{\partial}{\partial t} G_{\pm}^{(0)}(x, y; t) = -\frac{\partial}{\partial x} \left[-\frac{\partial}{\partial x} G_{\pm}^{(0)}(x, y; t) \pm F G_{\pm}^{(0)}(x, y; t) \right]. \quad (3)$$

The original probability density and the probability current are connected with their dimensionless counterparts by $\tilde{G}(\tilde{x}, \tilde{y}; \tilde{t}) = G(x, y; t)/L$ and $\tilde{J}(\tilde{x}, \tilde{y}; \tilde{t}) = k_B T J(x, y; t)/(\eta L^2)$.

Solution of the Fokker-Planck equations (3) runs along the standard lines [3]. After performing the Laplace transform, one arrives at the transformed functions $G_{\pm}^{(0)}(x, y; z)$ (here and below, the Laplace transformed functions are distinguished by quoting the complex variable z). Their explicit forms are given in the next section, cf. Eq. (10). They are then used as a starting point in the construction of the switching-averaged Green's functions. Alternatively, Eq. (3) can be solved by using spectral representation of the corresponding Fokker-Planck operators [11]. This procedure is reviewed in the Appendix A and it is then used as a basis for the numerical analysis of the potential-switching problem.

Let us now focus on the potential-switching process *per se*. As stated above, we assume that the process $Q(t)$ exhibits jumps at random time points $\{S_j\}_{j=1}^{\infty}$. Further, we assume that the waiting times in the two potential states $\{\tau_i\}_{i=2}^{\infty}$, $\tau_i = S_i - S_{i-1}$ form a system of mutually independent and identically distributed random variables. Differently speaking, we postulate that the switching times constitute a general *renewal process* [12]. Its definition will be completed by prescribing a generic probability density $f(t)$ for the waiting times $\{\tau_i\}_{i=2}^{\infty}$. For example, taking $f(t) = f_M(t) = \mu \exp(-\mu t)$, one arrives at the well known Poisson point process [12].

However, there is still one complication in the construction of the potential-switching process. Namely, in order to acquire a *stationary* stochastic process $Q(t)$ (which is a physically motivated requirement), two further conditions must be fulfilled. First, one has to take the symmetric initial condition $\text{Prob}\{Q(0) = \pm 1\} = 1/2$. Second, the *first* waiting time $\tau_1 = S_1$ must be controlled by the probability density $h(t) = [1 - F(t)]/m_1$, where $F(t) = \int_0^t dt' f(t')$ is the generic distribution function, and $m_1 = \int_0^{\infty} dt t f(t)$ is the first moment of the generic waiting time [12]. In the general case, $h(t)$ differs from the generic density $f(t)$. Notice that the Poisson point process plays an exceptional role in the sense that $h_M(t) = f_M(t)$ in this case.

Having guaranteed the stationarity of the switching process, its two time correlation function depends solely on the absolute value of the difference of its time arguments. Its Laplace transform is related to the Laplace transform of the generic probability density. Explicitly,

$$\langle Q(s+t)Q(s) \rangle = c(|t|), \text{ with } c(z) = \int_0^{\infty} dt e^{-zt} c(t) = \frac{1}{z} \left[1 - \frac{2\mu}{z} \frac{1-f(z)}{1+f(z)} \right], \quad (4)$$

where $\mu = 1/m_1$ is the mean frequency of the potential switching. For the Poisson point process, $c(t) = \exp(-2\mu t)$. Notice that the preparation of the stationary switching process necessitates a finite value of the mean switching time m_1 .

In concluding the section, let us emphasize the prominent role of the Poisson point process in the diffusion problem formulated above. Taking the exponentially distributed waiting times (this is just the case in the Doering-Gadoua paper [6]), the potential process $Q(t)$ is Markovian. On the other hand, even in this case, the particle position process $X(t)$ itself is non-Markovian. However, introducing an augmented description, i.e. describing the state of the system by the continuous particle position $X(t)$ and by the instantaneous value of the potential process $Q(t)$, the composite process $\{X(t), Q(t)\}$ will still be *Markovian* [2]. Consequently, the switching-averaged evolution operator for the unrestricted diffusion on the whole line $x \in (-\infty, +\infty)$ exhibits a time exponential form. Its explicit form has been derived in Ref. [13] and will be quoted below, c.f. Eqs. (37). In this case, the boundaries can be introduced *a posteriori* as a perturbation to the unrestricted diffusion in the fluctuating potential [13].

Summarizing, the exponential form of the generic probability density for the waiting times is a sufficient condition for the Markovian nature of the composite dynamics. However, the condition is also necessary. What happens if the waiting times are not exponentially distributed? In this case, even the composite dynamics is non-Markovian and the above procedure of affixing the boundaries to the unrestricted switching-averaged diffusion cannot be used. Instead, the boundary inclusion step must *precede* the potential-averaging procedure. We now turn to the detailed analysis of general non-Markovian cases.

III. THEORY

In this section, our primary objective is the calculation of the switching-averaged Green's functions. More precisely, the motion within the safe domain $x \in (0, 1)$ will be described by the state-of-potential resolved conditional densities

$G_{\alpha\beta}(x, y; t)$, defined as

$$G_{\alpha\beta}(x, y; t) dx = \text{Prob}\{X(t) \in (x, x + dx) \text{ and } Q(t) = \alpha \mid X(0) = y \text{ and } Q(0) = \beta\} , \quad (5)$$

with $\alpha, \beta = \pm$. The subscripts specify the final (α) and initial (β) state of the fluctuating potential while the arguments x, y give the final (x) and initial (y) position of the diffusing particle. Because of the absorbing boundary at $x = 0$ the total probability in the safe domain is not conserved. Instead, it gradually leaks out into the boundary. It is helpful to consider auxiliary quantities which describe the process of leaking of the probability out of the safe domain. We introduce the concept of the boundary channel, a hypothetical reservoir collecting the escaped probability into the absorbing boundary. We may even distinguish two boundary channels according to the state of the fluctuating potential at the moment of the absorption event. Therefore, the ‘plus’ boundary channel collects that part of the probability that escaped when the potential was in the state ‘plus’, and vice versa. In order to describe the dynamics of the channel filling processes, we introduce the boundary channel occupation Green’s functions. These quantities are given by

$$\pi_{\alpha\beta}(y; t) = \text{Prob}\{X(t) \in B_\alpha \mid X(0) = y \text{ and } Q(0) = \beta\} , \quad (6)$$

where the B_\pm denote the corresponding boundary channels. Again, the second subscript (β) relates to the initial state of the potential while the first (α) specifies the boundary channel in question. It is convenient to write these Green’s functions in the form of 2-by-2 matrices

$$\mathbf{G}(x, y; t) = \begin{pmatrix} G_{++}(x, y; t) & G_{+-}(x, y; t) \\ G_{-+}(x, y; t) & G_{--}(x, y; t) \end{pmatrix} , \quad \Pi(y; t) = \begin{pmatrix} \pi_{++}(y; t) & \pi_{+-}(y; t) \\ \pi_{-+}(y; t) & \pi_{--}(y; t) \end{pmatrix} . \quad (7)$$

Assume for a moment that the potential is static, i.e. it is fixed in one of its two states. Then the above matrices are diagonal and will play a role of unperturbed quantities

$$\mathbf{G}^{(0)}(x, y; t) = \begin{pmatrix} G_+^{(0)}(x, y; t) & 0 \\ 0 & G_-^{(0)}(x, y; t) \end{pmatrix} , \quad \Pi^{(0)}(y; t) = \begin{pmatrix} \pi_+^{(0)}(y; t) & 0 \\ 0 & \pi_-^{(0)}(y; t) \end{pmatrix} . \quad (8)$$

The Green’s function $\mathbf{G}^{(0)}(x, y; t)$ is given simply by the solutions to the Fokker-Planck equations (3) supplemented by the corresponding initial and boundary conditions. In the present dimensionless formulation, one starts with the equations

$$\frac{\partial G_\pm^0(x, y; t)}{\partial t} = \frac{\partial^2 G_\pm^0(x, y; t)}{\partial x^2} \mp F \frac{\partial G_\pm^0(x, y; t)}{\partial x} , \quad (9a)$$

with the initial conditions

$$G_\pm^0(x, y; t = 0) = \delta(x - y) , \quad (9b)$$

and the boundary conditions

$$G_\pm^0(0, y; t) = 0 , \quad \text{absorbing wall at } x = 0 , \quad (9c)$$

$$\left. \left(\frac{\partial}{\partial x} \mp F \right) G_\pm^0(x, y; t) \right|_{x=1} = 0 , \quad \text{reflecting wall at } x = 1 . \quad (9d)$$

After invoking the time Laplace transformation, one arrives at the explicit formulae

$$G_\pm^{(0)}(x, y; z) = \frac{1}{2D} \frac{e^{\pm \frac{F}{2}(x-y)}}{q_\pm e^{-D} - q_\mp e^D} \left[q_\pm e^{-D} (e^{D(x+y)} - e^{D|x-y|}) + q_\mp e^D (e^{-D(x+y)} - e^{-D|x-y|}) \right] . \quad (10)$$

where $D = \sqrt{(\frac{F}{2})^2 + z}$ and $q_\pm = \frac{F}{2} \pm D$.

The boundary channel occupation probabilities $\pi_\pm^{(0)}(y; t)$ are given by the probability conservation condition

$$\pi_\pm^{(0)}(y; t) = 1 - \int_0^1 dx G_\pm^{(0)}(x, y; t) . \quad (11)$$

This is a global conservation law for the probability. However, this law may be also put in a local form which we will find very useful in further manipulations. Namely, using the Fokker-Planck equations (9), the time derivative of the functions $\pi_{\pm}^{(0)}(y; t)$ can be rewritten as

$$\begin{aligned}\frac{\partial}{\partial t} \pi_{\pm}^{(0)}(y; t) &= -\frac{\partial}{\partial t} \int_0^1 dx G_{\pm}^{(0)}(x, y; t) = -\int_0^1 dx \left[\frac{\partial^2 G_{\pm}^{(0)}(x, y; t)}{\partial x^2} \mp F \frac{\partial G_{\pm}^{(0)}(x, y; t)}{\partial x} \right] \\ &= -\left(-\frac{\partial}{\partial x} \pm F \right) G_{\pm}^{(0)}(x, y; t) \Big|_{x=0} = \frac{\partial}{\partial x} G_{\pm}^{(0)}(x, y; t) \Big|_{x=0}.\end{aligned}\quad (12)$$

In the last two steps, we have used the assumed boundary conditions for Green's functions. The last but one expression gives a clear physical insight. The operator $-\frac{\partial}{\partial x} \pm F$ is the probability current operator for the corresponding slope of the potential. Thus, the equation (12) clearly states the local probability conservation law. Namely, the rate of the channel filling process equals the probability current into the absorbing boundary. Moreover, using Eq. (12), we can readily get the expression for $\pi_{\pm}^{(0)}(y; z)$. Taking the Laplace transform of (12), implementing the initial conditions $\pi_{\pm}^{(0)}(y; t=0) = 0$, and using (10), we obtain

$$\pi_{\pm}^{(0)}(y; z) = \frac{1}{z} \frac{\partial}{\partial x} G_{\pm}^{(0)}(x, y; z) \Big|_{x=0} = \frac{e^{\mp \frac{F}{2} y}}{z} \frac{q_{\pm} e^{-D(1-y)} - q_{\mp} e^{D(1-y)}}{q_{\pm} e^{-D} - q_{\mp} e^D}. \quad (13)$$

After these preparatory steps, let us focus on the construction of the full Green's functions for fluctuating potentials. Basically, our procedure consists of three steps. First, we shall assume an arbitrary fixed sequence of the potential-switching events and we shall follow the particle diffusion in the corresponding time dependent potential. Secondly, we attribute to any such evolution the probability weight of its realization. It is during this step that the properties of the underlying potential-switching process enter the calculation. Finally, we shall perform the averaging over the complete set of mutually exclusive evolutions. The averaged evolution is simply given by the sum over all possible evolutions weighted by the corresponding probabilities. This is a brief outline of the method of *construction of trajectories* introduced by Chvosta and Reineker in [10], where also the full formalism can be found.

Let us demonstrate the procedure on a simple example. Suppose that during the time interval $(0, t)$ there was just one switching event which occurred in the interval $(t_1, t_1 + dt_1)$. The weight of such a realization is simply $w_1(t, t_1, 0) dt_1 = [1 - F(t - t_1)] h(t_1) dt_1$. The corresponding evolution operator for the particle position within the safe domain reads $G_{\pm\pm}^{(1)}(x, y; t, t_1, 0) = 0$, $G_{\pm\mp}^{(1)}(x, y; t, t_1, 0) = \int_0^1 dx' G_{\pm}^{(0)}(x, x', t - t_1) G_{\mp}^{(0)}(x', y; t_1)$ which may be rewritten in the matrix form as

$$\mathbf{G}^{(1)}(x, y; t, t_1, 0) = \int_0^1 dx' \mathbf{G}^{(0)}(x, x'; t - t_1) \cdot \mathbf{S} \cdot \mathbf{G}^{(0)}(x', y; t_1), \quad (14a)$$

with the matrix $\mathbf{S} = \begin{pmatrix} 0 & 1 \\ 1 & 0 \end{pmatrix}$ representing the switching event. In the following, we will omit the spatial arguments x, y in Green's functions and we will use the matrix operator formalism in which the symbol ‘ \cdot ’ denotes the operator multiplication and the integration over x' . The above equation then reads

$$\mathbf{G}^{(1)}(t, t_1, 0) = \mathbf{G}^{(0)}(t - t_1) \cdot \mathbf{S} \cdot \mathbf{G}^{(0)}(t_1). \quad (14b)$$

To evaluate full Green's functions for the fluctuating potential we have to identify all possible evolution paths (trajectories) according to which the system may evolve, their respective weights, and finally sum up all those contributions of the kind shown in the above example. This may be done rather easily [10]

$$\begin{aligned}\mathbf{G}(t) &= (1 - H(t)) \mathbf{G}^{(0)}(t) + \int_0^t dt_1 (1 - F(t - t_1)) \mathbf{G}^{(0)}(t - t_1) \cdot \mathbf{S} \cdot h(t_1) \mathbf{G}^{(0)}(t_1) \\ &+ \int_0^t dt_1 \int_0^{t_1} dt_2 (1 - F(t - t_1)) \mathbf{G}^{(0)}(t - t_1) \cdot \mathbf{S} \cdot f(t_1 - t_2) \mathbf{G}^{(0)}(t_1 - t_2) \cdot \mathbf{S} \cdot h(t_2) \mathbf{G}^{(0)}(t_2) + \dots.\end{aligned}\quad (15)$$

The full evolution is represented as a sum of processes with zero, one, two, etc. potential switching events. We remind the definitions of the time distribution functions involved in the above formula: $F(t) = \int_0^t d\tau f(\tau)$, $h(t) = \frac{1}{m_1} [1 - F(t)]$, with $m_1 = \int_0^{\infty} dt t f(t)$, and $H(t) = \int_0^t d\tau h(\tau)$.

We also want to evaluate the boundary channel occupations, i.e. the boundary channel part of Green's function $\Pi(y; t)$. In this case one must be careful since the above procedure of the construction of trajectories does not yield the proper whole set of mutually exclusive paths for the evolution of $\Pi(y; t)$. However, for the time derivative $\frac{\partial}{\partial t} \Pi(y; t)$ the

above construction may be repeated since for this quantity the construction really provides the whole set of mutually exclusive trajectories as one may see by a closer inspection of them. Thus, a sample contribution analogous to the above one for the safe domain part of Green's function (14a) reads

$$\frac{\partial}{\partial t} \Pi^{(1)}(y; t, t_1, 0) = \int_0^1 dx' \frac{\partial}{\partial t} \Pi^{(0)}(x'; t - t_1) \cdot \mathbf{S} \cdot \mathbf{G}^{(0)}(x', y; t_1) = \frac{\partial}{\partial x} \mathbf{G}^{(1)}(x, y; t, t_1, 0) \Big|_{x=0}. \quad (16)$$

In the second step we used (12). Repeating the averaging procedure (15) for $\frac{\partial}{\partial t} \Pi(y; t)$ and bearing in mind (12) we derive this simple relation between the boundary channel occupation and the safe domain parts of Green's functions

$$\frac{\partial}{\partial t} \Pi(y; t) = \frac{\partial}{\partial x} \mathbf{G}(x, y; t) \Big|_{x=0}. \quad (17)$$

This formula expresses the local conservation law of probability for the composite diffusion and potential-fluctuation process.

The convolution structure of Green's function (15) enables to rewrite the above complicated time integrals structures via the Laplace transform into a simple geometrical series which may be formally summed up to the infinite order giving

$$\begin{aligned} \mathbf{G}(z) &= [(1 - H)\mathbf{G}^{(0)}](z) + [(1 - F)\mathbf{G}^{(0)}](z) \cdot \mathbf{S} \cdot [h\mathbf{G}^{(0)}](z) + [(1 - F)\mathbf{G}^{(0)}](z) \cdot \mathbf{S} \cdot [f\mathbf{G}^{(0)}](z) \cdot \mathbf{S} \cdot [h\mathbf{G}^{(0)}](z) + \dots \\ &= [(1 - H)\mathbf{G}^{(0)}](z) + [(1 - F)\mathbf{G}^{(0)}](z) \cdot (\mathbf{1} - \mathbf{S} \cdot [f\mathbf{G}^{(0)}](z))^{-1} \cdot \mathbf{S} \cdot [h\mathbf{G}^{(0)}](z) \\ &= [(1 - H)\mathbf{G}^{(0)}](z) + [(1 - F)\mathbf{G}^{(0)}](z) \cdot \mathbf{R}(z) \cdot \mathbf{S} \cdot [h\mathbf{G}^{(0)}](z), \end{aligned} \quad (18a)$$

$$\Pi(y; z) = \frac{1}{z} \frac{\partial}{\partial x} \mathbf{G}(x, y; z) \Big|_{x=0}. \quad (18b)$$

Structures like $[f\mathbf{G}^{(0)}](z) = \int_0^\infty dt e^{-zt} f(t) \mathbf{G}^{(0)}(t)$ mean a Laplace transform of the product. We introduced the quantity $\mathbf{R}(z)$ defined by

$$\mathbf{R}(z) = (\mathbf{1} - \mathbf{S} \cdot [f\mathbf{G}^{(0)}](z))^{-1} = \begin{pmatrix} 1 & -[f\mathbf{G}_-^{(0)}](z) \\ -[f\mathbf{G}_+^{(0)}](z) & 1 \end{pmatrix}^{-1} = \begin{pmatrix} \mathbf{I}_+(z) & [f\mathbf{G}_-^{(0)}](z) \cdot \mathbf{I}_-(z) \\ [f\mathbf{G}_+^{(0)}](z) \cdot \mathbf{I}_+(z) & \mathbf{I}_-(z) \end{pmatrix}, \quad (19)$$

with

$$\mathbf{I}_\pm(z) = \left(1 - [f\mathbf{G}_\mp^{(0)}](z) \cdot [f\mathbf{G}_\pm^{(0)}](z) \right)^{-1}. \quad (20)$$

Equations (18) are our main result for Green's functions of the composite process. In view of their importance, we rewrite them once more in an explicit form

$$\pi_{\alpha\beta}(y; z) = \frac{1}{z} \frac{\partial}{\partial x} G_{\alpha\beta}(x, y; z) \Big|_{x=0}, \quad (21)$$

with

$$\begin{aligned} G_{++}(x, y; z) &= [(1 - H)G_+^{(0)}](x, y; z) \\ &+ \int_0^1 dx_1 \int_0^1 dx_2 \int_0^1 dx_3 [(1 - F)G_+^{(0)}](x, x_1; z) \cdot [fG_-^{(0)}](x_1, x_2; z) \cdot \mathbf{I}_-(x_2, x_3; z) \cdot [hG_+^{(0)}](x_3, y; z), \end{aligned} \quad (22a)$$

$$G_{-+}(x, y; z) = \int_0^1 dx_1 \int_0^1 dx_2 [(1 - F)G_-^{(0)}](x, x_1; z) \cdot \mathbf{I}_-(x_1, x_2; z) \cdot [hG_+^{(0)}](x_2, y; z), \quad (22b)$$

$$G_{+-}(x, y; z) = \int_0^1 dx_1 \int_0^1 dx_2 [(1 - F)G_+^{(0)}](x, x_1; z) \cdot \mathbf{I}_+(x_1, x_2; z) \cdot [hG_-^{(0)}](x_2, y; z), \quad (22c)$$

$$\begin{aligned} G_{--}(x, y; z) &= [(1 - H)G_-^{(0)}](x, y; z) \\ &+ \int_0^1 dx_1 \int_0^1 dx_2 \int_0^1 dx_3 [(1 - F)G_-^{(0)}](x, x_1; z) \cdot [fG_+^{(0)}](x_1, x_2; z) \cdot \mathbf{I}_+(x_2, x_3; z) \cdot [hG_-^{(0)}](x_3, y; z), \end{aligned} \quad (22d)$$

where the quantities $I_{\pm}(x, y; z)$ are determined by the following integral equations of the Lipmann-Schwinger kind

$$I_{\pm}(x, y; z) = \delta(x - y) + \int_0^1 dx' K_{\pm}(x, x'; z) \cdot I_{\pm}(x', y; z) , \quad (22e)$$

with the kernels $K_{\pm}(x, y; z)$ being

$$K_{\pm}(x, y; z) = \int_0^1 dx' [fG_{\mp}^{(0)}](x, x'; z) \cdot [fG_{\pm}^{(0)}](x', y; z) . \quad (22f)$$

Obviously enough, solutions of the integral equations (22e) form the crucial point of the whole procedure. Solving them we also get the boundary channel occupations $\pi_{\alpha\beta}(y; z)$ given by (21) which yield the complete information about the absorption process, i.e. they fully describe the time evolution of the probability captured in the individual boundary channels.

In the following, we restrict ourselves mostly to a reduced information concerning the boundary channel occupations. Namely, we will consider the asymptotic boundary channel occupation quantities defined as

$$P_{\alpha\beta}(y) = \lim_{t \rightarrow \infty} \pi_{\alpha\beta}(y; t) = \lim_{z \rightarrow 0} z \pi_{\alpha\beta}(y; z) , \quad (\text{ABCO}), \quad (23)$$

and also the first moments of the boundary channels occupation densities reading

$$\tau_{\alpha\beta}(y) = \int_0^{\infty} dt t \frac{d\pi_{\alpha\beta}(y; t)}{dt} = \lim_{z \rightarrow 0} \frac{P_{\alpha\beta}(y) - z \pi_{\alpha\beta}(y; z)}{z} . \quad (24)$$

These quantities are simply related to the mean first passage times $\tau_{\pm}(y)$ for respective initial conditions $Q(0) = \pm$ by

$$\tau_{\pm}(y) = \tau_{+\pm}(y) + \tau_{-\pm}(y) , \quad (\text{MFPT}). \quad (25)$$

IV. DISCUSSION

A. Markovian Case Revisited

In this subsection we use the general formalism developed in the previous section and apply it to the Markovian case studied already in [6] by Doering and Gadoua. We revisit this case in order to show the equivalence of our approach to the standard one in the Markovian case and also to state new results for the boundary occupation probability densities which are easily obtained within our formalism.

For the Markovian case, the waiting time distribution functions are $f(t) = h(t) = f_M(t) = \mu e^{-\mu t}$, $1 - F(t) = 1 - H(t) = e^{-\mu t} = \frac{f(t)}{\mu}$. The Laplace transform of $f(t)$ is $f(z) = \frac{\mu}{z + \mu}$ and for any function $G(t)$ the following identity holds $[fG](z) = \int_0^{\infty} dt e^{-zt} f(t)G(t) = \mu G(z + \mu)$. We use these properties in (18) to obtain

$$\mathbf{G}(z) = [(1 - F)\mathbf{G}^0](z) \cdot (\mathbf{1} + \mathbf{R}(z) \cdot \mathbf{S} \cdot [f\mathbf{G}^0](z)) = \mathbf{G}^0(z + \mu) \cdot \mathbf{R}(z) , \quad (26)$$

where we have taken into account that $\mathbf{R}(z) = (\mathbf{1} - \mathbf{S} \cdot [f\mathbf{G}^0](z))^{-1}$, cf. Eq. (19). We further use

$$\begin{aligned} \mathbf{R}(z) &= \begin{pmatrix} 1 & -[fG_{-}^0](z) \\ -[fG_{+}^0](z) & 1 \end{pmatrix}^{-1} = \left[\begin{pmatrix} [fG_{+}^0](z)^{-1} & -1 \\ -1 & [fG_{-}^0](z)^{-1} \end{pmatrix} \cdot \begin{pmatrix} [fG_{+}^0](z) & 0 \\ 0 & [fG_{-}^0](z) \end{pmatrix} \right]^{-1} \\ &= \mathbf{G}^0(z + \mu)^{-1} \cdot \begin{pmatrix} G_{+}^0(z + \mu)^{-1} & -\mu \\ -\mu & G_{-}^0(z + \mu)^{-1} \end{pmatrix}^{-1} . \end{aligned} \quad (27)$$

Thus, for Green's function in the safe domain $\mathbf{G}(z)$, we simply get the matrix Fokker-Planck equation valid for the Markovian switching process (cf. Eq. (4) in [6]) and defined by

$$\begin{pmatrix} G_{+}^0(z + \mu)^{-1} & -\mu \\ -\mu & G_{-}^0(z + \mu)^{-1} \end{pmatrix} \cdot \mathbf{G}(z) = \mathbf{1} , \quad (28a)$$

which reads, in the x -representation,

$$\begin{pmatrix} z + \mu - \frac{\partial^2}{\partial x^2} + F \frac{\partial}{\partial x} & -\mu \\ -\mu & z + \mu - \frac{\partial^2}{\partial x^2} - F \frac{\partial}{\partial x} \end{pmatrix} \cdot \mathbf{G}(x, y; z) = \delta(x - y) \mathbf{1} , \quad (28b)$$

supplemented with the appropriate boundary conditions

$$\left(\begin{pmatrix} \frac{\partial}{\partial x} - F & 0 \\ 0 & \frac{\partial}{\partial x} + F \end{pmatrix} \cdot \mathbf{G}(x, y; z) \right) \Big|_{x=1} = \mathbf{0} , \quad (28c)$$

$$\mathbf{G}(x, y; z) \Big|_{x=0} = \mathbf{0} . \quad (28d)$$

We may proceed further to analytically evaluate $\pi_{ij}(y; z)$ using (21) from the knowledge of the Markovian Green's function which may be expressed as

$$\mathbf{G}(x, y; z) = \mathbf{G}_R(x, y; z) - \mathbf{G}_R(x, 0; z) \cdot \mathbf{G}_R^{-1}(0, 0; z) \cdot \mathbf{G}_R(0, y; z) , \quad \text{for all } x, y \in (0, 1) , \quad (29)$$

where $\mathbf{G}_R(x, y; z)$ is Green's function solving equation (28b) on $(-\infty, 1)$ with the reflecting boundary condition (28c) at $x = 1$. It is readily verified that Green's function $\mathbf{G}(x, y; z)$ expressed in this way satisfies indeed all necessary conditions including the absorbing boundary condition (28d) at $x = 0$. For any Green's function satisfying (28b), the following identities hold (cf. [14], Chap. 2.3, here the identities are applied to $\mathbf{G}_R(x, y; z)$)

$$\mathbf{G}_R(x, y; z) = \mathbf{G}_R(x, x'; z) \cdot \mathbf{G}_R^{-1}(x', x'; z) \cdot \mathbf{G}_R(x', y; z) , \quad \text{with } x \leq x' \leq y < 1 , \quad (30)$$

and

$$\frac{\partial}{\partial x} \mathbf{G}_R(x, y; z) \Big|_{x=y+0} - \frac{\partial}{\partial x} \mathbf{G}_R(x, y; z) \Big|_{x=y-0} = -\mathbf{1} , \quad \text{for all } y < 1 . \quad (31)$$

Putting (29) in (21) while expressing the first term via (30) as

$$\frac{\partial}{\partial x} \mathbf{G}_R(x, y; z) \Big|_{x=0} = \frac{\partial}{\partial x} \mathbf{G}_R(x, \epsilon; z) \Big|_{x=0} \cdot \mathbf{G}_R^{-1}(\epsilon, \epsilon; z) \cdot \mathbf{G}_R(\epsilon, y; z) , \quad \text{for } 0 < \epsilon < y < 1 , \quad (32)$$

and taking the limit $\epsilon \rightarrow 0+$ together with (31) we obtain

$$\pi(y; z) = \frac{1}{z} \mathbf{G}_R^{-1}(0, 0; z) \cdot \mathbf{G}_R(0, y; z) , \quad \text{for all } y \in (0, 1) . \quad (33)$$

Now, we can follow the same procedure to evaluate 'reflecting' Green's function $\mathbf{G}_R(x, y; z)$ in terms of Green's function acting in the unrestricted real axis $(-\infty, \infty)$ which we denote by $\mathbf{G}_\infty(x, y; z)$. The analogy of the formula (29) for $\mathbf{G}_R(x, y; z)$ reads

$$\mathbf{G}_R(x, y; z) = \mathbf{G}_\infty(x, y; z) - \mathbf{G}_\infty(x, 1; z) \cdot [\mathcal{R}\mathbf{G}_\infty(1^-, 1; z)]^{-1} \cdot \mathcal{R}\mathbf{G}_\infty(1, y; z) , \quad \text{for all } x, y < 1 , \quad (34)$$

where $\mathcal{R}\mathbf{G}_\infty(x, y; z)$ denotes

$$\mathcal{R}\mathbf{G}_\infty(x, y; z) = \begin{pmatrix} \frac{\partial}{\partial x} - F & 0 \\ 0 & \frac{\partial}{\partial x} + F \end{pmatrix} \cdot \mathbf{G}_\infty(x, y; z) . \quad (35)$$

For the initial condition $y = 1$ considered by Doering and Gadoua we may further simplify the final result for the boundary channel occupation (33). Putting (34) into (33) with $y \rightarrow 1^-$ and using the analogy of Eq. (31) for $\mathbf{G}_\infty(x, y; z)$ we come to the result

$$\pi(1; z) = \frac{1}{z} [\mathcal{R}\mathbf{G}_\infty(1^-, 1; z) \cdot \mathbf{G}_\infty^{-1}(0, 1; z) \cdot \mathbf{G}_\infty(0, 0; z) - \mathcal{R}\mathbf{G}_\infty(1, 0; z)]^{-1} . \quad (36)$$

The ingredient Green's function $\mathbf{G}_\infty(x, y; z)$ can be evaluated easily via the Fourier transform of (28b) with the result [13]

$$\mathbf{G}_\infty(x, y; z) = \begin{pmatrix} g_{++}(x, y; z) & g_{+-}(x, y; z) \\ g_{-+}(x, y; z) & g_{--}(x, y; z) \end{pmatrix} , \quad (37a)$$

where $g_{ij}(x, y; z)$ are given by

$$g_{++}(x, y; z) = \frac{1}{g(z)} [\theta(x - y) f^<(x, y; z) + \theta(y - x) f^>(x, y; z)] , \quad (37b)$$

$$g_{--}(x, y; z) = \frac{1}{g(z)} [\theta(x - y) f^>(x, y; z) + \theta(y - x) f^<(x, y; z)] , \quad (37c)$$

$$g_{+-}(x, y; z) = g_{-+}(x, y; z) = \frac{\mu}{g(z)} [u_+(z) e^{-u_-(z)|x-y|} - u_-(z) e^{-u_+(z)|x-y|}] , \quad (37d)$$

with the following notation

$$u_{\pm}(z) = \sqrt{z + \mu + \frac{F^2}{2} \pm \sqrt{\left(z + \mu + \frac{F^2}{2}\right)^2 - z(z + 2\mu)}} , \quad (37e)$$

$$g(z) = 2u_+(z)u_-(z)[u_+^2(z) - u_-^2(z)] , \quad (37f)$$

$$f^<(x, y; z) = u_+(z)\beta_-(z)e^{-u_-(z)|x-y|} - u_-(z)\beta_+(z)e^{-u_+(z)|x-y|} , \quad (37g)$$

$$f^>(x, y; z) = u_+(z)\gamma_-(z)e^{-u_-(z)|x-y|} - u_-(z)\gamma_+(z)e^{-u_+(z)|x-y|} , \quad (37h)$$

$$\beta_{\pm} = z + \mu - u_{\pm}^2(z) + Fu_{\pm}(z) , \quad (37i)$$

$$\gamma_{\pm} = z + \mu - u_{\pm}^2(z) - Fu_{\pm}(z) . \quad (37j)$$

Introducing these expressions into (36), we obtain the final result for the boundary channel occupation in the Markovian case. To accomplish this task we had to use the symbolic manipulations program Maple. Instead of quoting the full rather involved result, we only present the physically transparent expression for ABCO

$$P_{++}(1) = \frac{\mu k \cosh(k) - \mu F \sinh(k) + \mu k(1 + F) + kF^2}{k(2\mu \cosh(k) + F^2)} , \quad (38a)$$

$$P_{-+}(1) = \frac{\mu(k \cosh(k) + F \sinh(k) - k(1 + F))}{k(2\mu \cosh(k) + F^2)} , \quad (38b)$$

$$P_{+-}(1) = \frac{\mu(k \cosh(k) - F \sinh(k) - k(1 - F))}{k(2\mu \cosh(k) + F^2)} , \quad (38c)$$

$$P_{--}(1) = \frac{\mu k \cosh(k) + \mu F \sinh(k) + \mu k(1 - F) + kF^2}{k(2\mu \cosh(k) + F^2)} , \quad (38d)$$

with $k = \sqrt{2\mu + F^2}$ being the exact analog of (10c) in [6] in our dimensionless quantities. One can easily see that the probability conservation conditions for asymptotic times $P_{++} + P_{-+} = 1$ and $P_{+-} + P_{--} = 1$ are satisfied. Doering and Gadoua considered the MFPT for the symmetric initial condition $\text{Prob}\{Q(0) = \pm\} = \frac{1}{2}$ and $y = 1$. This quantity is just $\tau(1) = \frac{\tau_+(1) + \tau_-(1)}{2}$, cf. Eq. (25). We calculated it too using our method and explicitly compared it, with the help of Maple, with the Doering's and Gadoua's famous result (10a-c). We came to exactly the same expression. Moreover, we give here the analytic expression for ABCO for the 'minus' channel, a quantity analogous to that depicted in Fig. 4 of [6] as a result of the Monte Carlo simulation (for that calculation, DG used the potential switching between $F_+ = 8$ and $F_- = 0$)

$$P_-(1) = \frac{P_{-+}(1) + P_{--}(1)}{2} = \frac{2\mu k \cosh k + 2\mu F \sinh(k) - 2\mu F k + kF^2}{2k(2\mu \cosh(k) + F^2)} . \quad (39)$$

The curves of $P_-(1)$, $\tau(1)$ as functions of μ for $F = 8$ are plotted in Fig. 2 for reference to be compared with other results generated by non-Markovian switching.

B. Non-Markovian Cases

In this subsection, we present the results for several non-Markovian switching processes generated by various renewal processes. The waiting time probability densities and other characteristics of the renewal processes used in our calculations are summarized in Table I, and the nonsingular densities are also plotted in Fig. 1. In order to

compare the ABCO and MFPT curves for different potential switching processes, we normalized all waiting time densities (except for one which cannot be normalized) so that the mean switching time equals $\frac{1}{\mu}$, i.e. $\int_0^\infty dt t f(t) = \frac{1}{\mu}$. Further, the probability normalization condition implies that $\int_0^\infty dt f(t) = 1$.

We evaluated the ABCO of the ‘minus’ channel and the MFPT for the symmetric initial condition $\text{Prob}\{Q(0) = \pm\} = \frac{1}{2}$ and $y = 1$ considered also in the Markovian case. These quantities are defined as follows. The ABCO for the ‘minus’ channel is

$$P_-(1) = \frac{P_{-+}(1) + P_{--}(1)}{2} \quad (40)$$

(cf. Eq. (23)) while the MFPT $\tau(1)$ reads

$$\tau(1) = \frac{\tau_+(1) + \tau_-(1)}{2} = \frac{1}{2} \sum_{\alpha, \beta = \pm} \tau_{\alpha\beta}(1) \quad (41)$$

(cf. Eq. (24)).

To calculate these quantities we used a numerical solution of (21) and (22). The details of the numerical calculations are explained in the Appendix ???. It is of interest to mention that for some specific waiting time distributions like Γ_n distributions used below, it would be possible to write down and solve in an analytic form the equations for Green’s functions analogous to (28b). However, we decided to solve all the non-Markovian cases numerically in this paper.

In the first set of pictures, Fig. 2, we plot the results for the ABCO and MFPT for the processes generated by waiting time distributions decaying fast for $t \rightarrow \infty$. The waiting time distributions used here cover the Γ_n distributions with $n = 0$ (Markovian case), 1 and 5, the delta-function distribution corresponding to the deterministic switching process, and a two-delta-function distribution. All these functions are strongly damped for large t , they all decay faster than an exponential, the delta-function distributions even have a compact support. With increasing n , the Γ_n distributions are better localized around $\frac{1}{\mu}$ and, thus, the switching time is closer to this mean switching time. This behaviour finally results in the deterministic switching in the $n = \infty$ case. We also considered the two-delta-function distribution whose double peak structure is qualitatively distinct from the single peak of all Γ_n distributions. The value of the variance of this density lies between the Γ_1 and Γ_5 cases.

In the figures depicting the ABCO and MFPT quantities one can see that the qualitative features of the Markov case are preserved even for the considered non-Markovian switching potentials. Namely, both the wide resonant activation maximum in the ABCO curve as well as the resonant activation minimum in the MFPT curve are present in all cases. Compared with the Markovian case the resonant extremes are more pronounced and slightly shifted towards lower switching frequencies with decreasing variance of the density, i.e. with sharper switching time distribution. This behaviour is better observable for the MFPT curve and is apparently just the consequence of the still better time localization of the switching events. The obtained results support the interpretation that the form of the resonant extremes depends predominantly on the variance of the switching time probability density and not on the detailed fine structure of the density (compare Γ_1 , two-delta-functions, and Γ_5 cases).

To verify the numerical representation of the analytic expressions (21) and (22), we performed Monte Carlo simulations by which we reproduced explicitly the construction of trajectories method. The simulation technique is briefly surveyed at the end of the Appendix ???. In Fig. 3, we give the results for the deterministic switching case which we chose as representative of non-Markovian processes. To this end we performed 250 000 runs of the simulation. In the figures, there are presented the results of the numerical solution to the analytical formulas for the ABCO and MFPT together with the corresponding quantities obtained by the simulations. As we can see our analytical solution is fully justified by the results of simulations. We also included in the figures the curves for a modified process generated by a non-stationary switching process with the first switching time distribution equal to all others $h(t) = f(t)$. By this, we wanted to demonstrate the influence of the initial condition on the absorption process. Since for high enough switching frequencies the curves collapse for both the stationary and non-stationary case, we see that for these high frequencies the initial conditions are forgotten and do not influence the absorption process. It is plausible that this behaviour occurs for frequencies higher than the inverse of the mean first passage time for the negative slope of the potential which means $\mu \gtrsim \tau_-^{-1} = \frac{F^2}{e^{-F} - 1 + F} \approx 10$. This behaviour of forgetting the initial conditions was also observed for other so far considered non-Markovian processes (not shown). The same applies for an alternate modification of the initial condition by considering non-symmetric probability for the initial state of the potential slope.

We also performed the calculations for the waiting time distributions decaying slowly for large t . Namely, we considered the distributions decaying like power laws, i.e. $f(t) = f_\alpha(t) \propto t^{-\alpha}$ with $\alpha = \frac{3}{2}, \frac{5}{2}, \frac{7}{2}$ for large t . The exact expressions for these densities are shown in Table I and these functions are also shown in Fig. 1. The peculiarities of these densities compared with the previously considered ones are in the absence of higher order moments which means that integrals of the kind $\int_0^\infty dt t^k f(t)$ diverge for integer $k \geq \alpha - 1$. The distributions chosen above do not have

moments starting from the first, the second, and the third, respectively. The results for these distributions, together with their non-stationary counterparts (for the $\alpha = \frac{3}{2}$ case, only the non-stationary results are stated), are shown in Fig. 4. Moreover, we also present there the results of the Monte Carlo simulations for the $\alpha = \frac{5}{2}$ stationary case.

One can see that the results for the $\alpha = \frac{7}{2}$ case are qualitatively the same as for Γ_n like distributions including the property of forgetting the initial conditions. On the other hand, the cases of $\alpha = \frac{3}{2}$ and $\frac{5}{2}$ are completely different in their behaviour. Let us first consider the $\alpha = \frac{5}{2}$ case. We see that the curves for the two different initial conditions (stationary vs. non-stationary cases) do not collapse for high frequencies and, what is even more striking, the curve corresponding to the stationary case does not exhibit the resonance activation minimum at all. We tried to verify our results for this interesting case by simulations, however due to the fact that these simulations were very numerically demanding we were not able to cover all the frequency range. Nevertheless, the results obtained allow us to extrapolate that the resonant minimum of the MFPT curve is indeed absent in this stationary case. On the other hand the non-stationary case seems to still exhibit shallow resonant activation minimum. As we already mentioned the high frequency behaviours of these two cases are different, but the limiting values of both when $\mu \rightarrow \infty$ are apparently the same. Even this feature is not preserved in the $\alpha = \frac{3}{2}$ case. In this case both the ABCO and MFPT curves are very different from all previous ones, namely even the asymptotic behaviour for high frequencies does not converge to the customary value of the averaged potential. This behaviour is obviously caused by the divergence of the mean switching time. It is hard to conclude whether a very shallow resonant minimum of the MFPT curve is present or not.

All these findings open up the discussion about conditions under which the resonance activation phenomenon demonstrated by the minimum of the MFPT curve occurs. We saw that for all waiting time distributions having at least the first two moments which generate the potential switching process this phenomenon was present, while we found an interesting possibility that it is absent for potential switching processes generated by long tail distributions, namely distributions without second moment. The processes generated by these distributions also depend on the initial conditions even for high frequencies and for the distribution without the first moment even the high frequency asymptotics is non-standard. Both these properties seem to be attributable to the absence of the second or first moment of the density. Since the densities without second moment occur in nature quite generically, e.g. Lévy ones, we draw the attention to this issue. To our knowledge, in all previous calculations there have been used the Markovian or deterministic (in the context of coherent stochastic resonance) potential switching processes. However, as we have just shown, there is a whole class of potential switching processes generated by such long tail waiting time distributions for which the Markovian like class results are incorrect.

V. CONCLUSIONS

We have developed a general method for studying the resonant activation phenomenon in non-Markovian fluctuating potentials generated by a general renewal process. We have applied this method to the generalization of the model considered previously by Doering and Gadoua. We have considered several non-Markovian waiting time distributions of the underlying renewal process. Namely, we have found the asymptotic boundary channel occupation and mean first passage time for potential-fluctuation processes generated by fast decaying waiting time probability densities (Γ_n distributions, deterministic switching, two-delta functions) and by asymptotically power law densities without the first, the second, and the third moment (and all higher moments), respectively.

It has been found that for all densities having at least the first two moments the resonance activation phenomenon is present and the curves for the MFPT as well as for the ABCO are qualitatively the same. Moreover, the quantitative results suggest that the relevant quantity governing the precise structure of these curves is the variance of the waiting time probability densities. We have drawn the conclusion that the smaller the variance the better is the resonant activation minimum developed. Indeed, the best developed minimum can be found on the curve corresponding to the (non-stationary) deterministic case with zero variance while the minima in other cases are more shallow in a good accord with the increasing variance, cf. Table I. The depth of the minimum at the logarithmic scale for the deterministic case is about twice as much as for the $\alpha = \frac{7}{2}$ or Markovian cases. It would definitely be of importance to check what consequences such a change may have for physically more relevant models like Brownian motors.

On the other hand, we have realized that, for waiting time densities which do not have the second or even the first moment, the resonant activation phenomenon is absent and the model exhibits other peculiar features, e.g. a strong dependence on the initial conditions, or a non-standard high-switching-frequency asymptotic behaviour. The probability densities not having these moments are quite common in nature, as exemplified by the Lévy ones. We would like to stress that these results may be of a direct physical importance, for example, in biophysical studies. We plan to explore the behaviour of the processes generated by such densities in more detail in the future.

The method used can be extended in many ways. More general potential profiles and boundary conditions may be accounted for in a straightforward manner, allowing for studies of physically relevant systems like surmounting real

barriers or Brownian-motor-like setups. The extension to the fluctuating potentials with more than two states was already formulated in an abstract manner in [10]. Special instances of this extension have been used independently in the coherent stochastic resonance problems [9], where the harmonic driving is approximated by a multistep periodic signal. Thus, the generalization of our model to more potential states together with taking into account the appropriate boundary conditions (absorbing traps at both ends of the interval) would be directly applicable in a generalized coherent stochastic resonance context. As we mentioned already, it is also possible to find the analytic solution to our present model for suitable waiting time densities the best candidate of which is the Γ_1 distribution. This is being considered presently too.

Acknowledgments

We want to thank Professor B. Velický for stimulating discussions and for his help with the preparation of this manuscript.

[1] N. G. van Kampen, *Stochastic Processes in Physics and Chemistry* (North-Holland, 1992).
 [2] C. W. Gardiner, *Handbook of Stochastic Methods* (Springer, 1985), second ed.
 [3] H. Risken, *The Fokker-Planck Equation* (Springer, 1989).
 [4] P. Reimann and P. Hänggi, in *Stochastic Dynamics*, edited by L. Schimansky-Geier and T. Pöschel (Springer, Berlin, 1997), no. 484 in Lecture Notes in Physics, pp. 127–139.
 [5] L. Gammaitoni, P. Hänggi, P. Jung, and F. Marchesoni, Rev. Mod. Phys. **70**(1), 223 (1998).
 [6] C. R. Doering and J. C. Gadoua, Phys. Rev. Lett. **69**(16), 2318 (1992).
 [7] J. Maddox, Nature **359**, 771 (1992).
 [8] J. M. Porra, Phys. Rev. E **55**(6), 6533 (1997).
 [9] A. K. Dhara and T. Mukhopadhyay, Phys. Rev. E **60**(3), 2727 (1999).
 [10] P. Chvosta and P. Reineker, Physica A **268**, 103 (1999).
 [11] M. Mörsch, H. Risken, and H. D. Vollmer, Z. Physik B **32**, 245 (1979).
 [12] D. R. Cox, *Renewal Theory* (Wiley, New York, 1962).
 [13] P. Chvosta and N. Pottier, Physica A **255**, 332 (1998).
 [14] F. García-Moliner and V. R. Velasco, *Theory of Single and Multiple Interfaces* (World Scientific, Singapore, 1992).

Designation	Type	Density	Laplace transform	Mean	Variance
Γ_n	gamma	$f_{\Gamma_n}(t) = \mu \frac{(n+1)^{(n+1)}}{n!} (\mu t)^n e^{-(n+1)\mu t}$	$f_{\Gamma_n}(z) = \left[1 + \frac{z}{(n+1)\mu}\right]^{-(n+1)}$	$\frac{1}{\mu}$	$\frac{1}{(n+1)\mu^2}$
Γ_0 (Markov)	gamma	$f_M(t) = \mu e^{-\mu t}$	$f_M(z) = \left(1 + \frac{z}{\mu}\right)^{-1}$	$\frac{1}{\mu}$	$\frac{1}{\mu^2}$
Γ_1	gamma	$f_{\Gamma_1}(t) = 4\mu^2 t e^{-2\mu t}$	$f_{\Gamma_1}(z) = \left(1 + \frac{z}{2\mu}\right)^{-2}$	$\frac{1}{\mu}$	$\frac{1}{2\mu^2}$
Γ_5	gamma	$f_{\Gamma_5}(t) = \frac{1944}{5} \mu^6 t^5 e^{-6\mu t}$	$f_{\Gamma_5}(z) = \left(1 + \frac{z}{6\mu}\right)^{-6}$	$\frac{1}{\mu}$	$\frac{1}{6\mu^2}$
δ (determ.)	one-point	$f_\delta(t) = \delta(t - \frac{1}{\mu})$	$f_\delta(z) = e^{-\frac{z}{\mu}}$	$\frac{1}{\mu}$	0
2δ	two-point	$f_{2\delta}(t) = \frac{1}{2} \delta(t - \frac{1}{2\mu}) + \frac{1}{2} \delta(t - \frac{3}{2\mu})$	$f_{2\delta}(z) = \frac{1}{2} e^{-\frac{z}{2\mu}} (1 + e^{-\frac{z}{\mu}})$	$\frac{1}{\mu}$	$\frac{1}{4\mu^2}$
$\alpha = \frac{3}{2}$	power law	$f_{3/2}(t) = \frac{1}{\sqrt{2\pi\mu^3 t^3}} e^{-\frac{1}{2\mu t}}$	$f_{3/2}(z) = e^{-\sqrt{\frac{2z}{\mu}}}$	∞	∞
$\alpha = \frac{5}{2}$	power law	$f_{5/2}(t) = \frac{1}{\sqrt{2\pi\mu^3 t^5}} e^{-\frac{1}{2\mu t}}$	$f_{5/2}(z) = (1 + \sqrt{\frac{2z}{\mu}}) e^{-\sqrt{\frac{2z}{\mu}}}$	$\frac{1}{\mu}$	∞
$\alpha = \frac{7}{2}$	power law	$f_{7/2}(t) = \frac{3\sqrt{3}}{\sqrt{2\pi\mu^5 t^7}} e^{-\frac{3}{2\mu t}}$	$f_{7/2}(z) = (1 + \frac{2z}{\mu} + \sqrt{\frac{6z}{\mu}}) e^{-\sqrt{\frac{6z}{\mu}}}$	$\frac{1}{\mu}$	$\frac{2}{\mu^2}$

TABLE I: List of waiting time probability densities used in the calculations. All densities are normalized to one. In order to allow the direct comparison between the individual cases, all densities are scaled to yield the same mean waiting time $\frac{1}{\mu}$ (except for the $\alpha = \frac{3}{2}$ case, where the corresponding integral diverges). The first entry describes the general properties of the generic Γ_n distribution of which the next three ones are just special cases. The deterministic case can be also viewed as a particular case of Γ_n distribution since it is a limit of it when $n \rightarrow \infty$. The power law cases (last three entries) are specific by the lack of higher order moments. Our representatives does not have moments starting from the first, the second and the third, respectively. It is the reason why the $\alpha = \frac{3}{2}$ case cannot be normalized to the common mean value. Yet, we use a similar scaling like in all other cases so that $\frac{1}{\mu}$ acts as some ‘typical time’ characterizing the shape of this density. In stationary cases also the Laplace transforms of the modified densities $h(t)$ were used in the calculations. They can be easily obtained from $f(z)$ as $h(z) = \mu \frac{1-f(z)}{z}$. The nonsingular densities are plotted in Fig. 1.

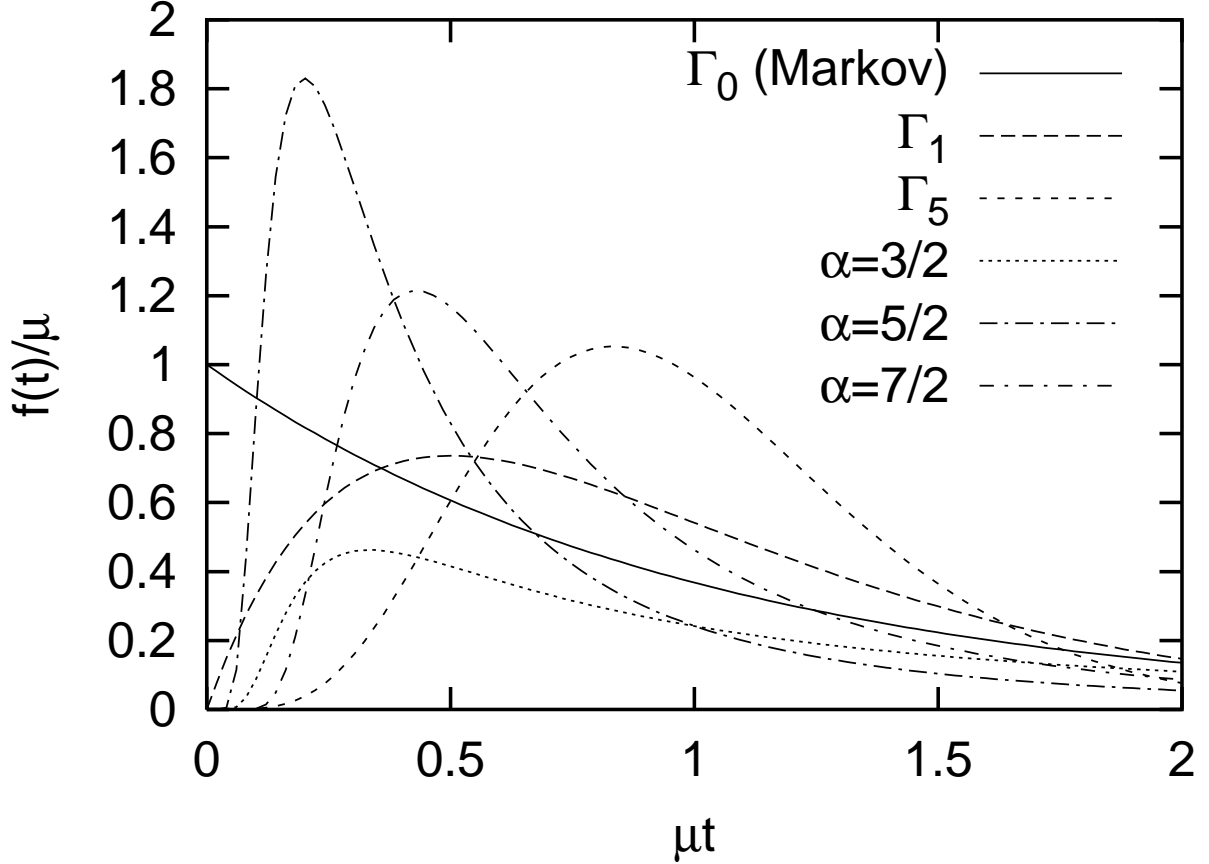


FIG. 1: Probability densities of waiting times for different switching processes. The curves correspond to Γ_n distributions with $n = 0$ (Markovian case) (solid line), $n = 1$ (long dashed line), and $n = 5$ (short dashed line) and to asymptotically power law distributions with $\alpha = \frac{3}{2}$ (dotted line), $\alpha = \frac{5}{2}$ (long dash-dotted line), and $\alpha = \frac{7}{2}$ (short dash-dotted line).

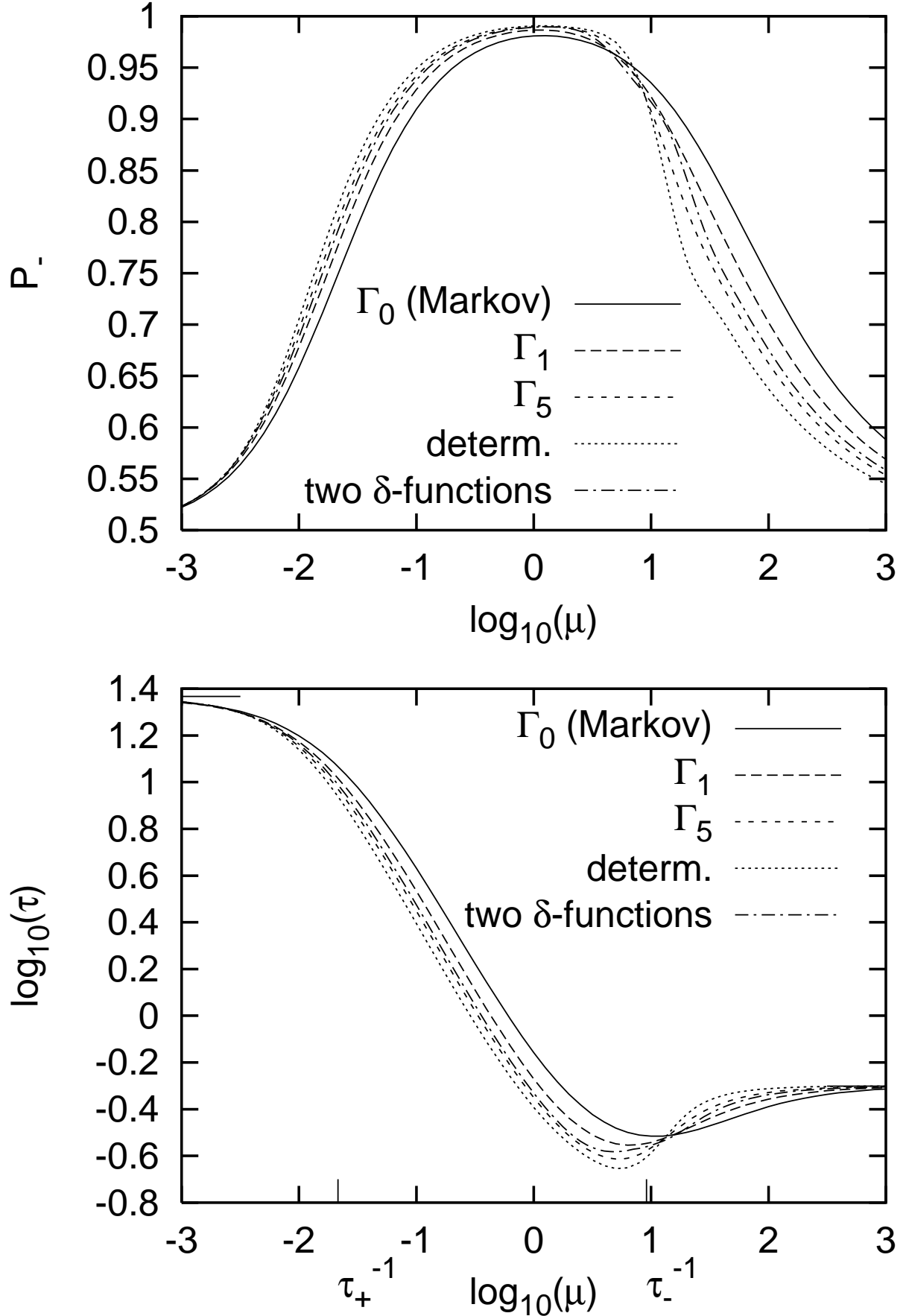


FIG. 2: ABCO and MFPT for waiting times distributions with fast decay for $t \rightarrow \infty$, namely, Γ_0 (Markovian case) (solid line), Γ_1 (long dashed line), Γ_5 (short dashed line), deterministic switching (dotted line), and two δ -functions distribution (dot-dashed line). The τ_{\pm} denote the mean first passage times for the respective slopes of the potential. The limiting values of MFPT in the static limit (the average of both τ 's) and in the infinitely fast switching limit (motion in the average potential) are also shown by the bars.

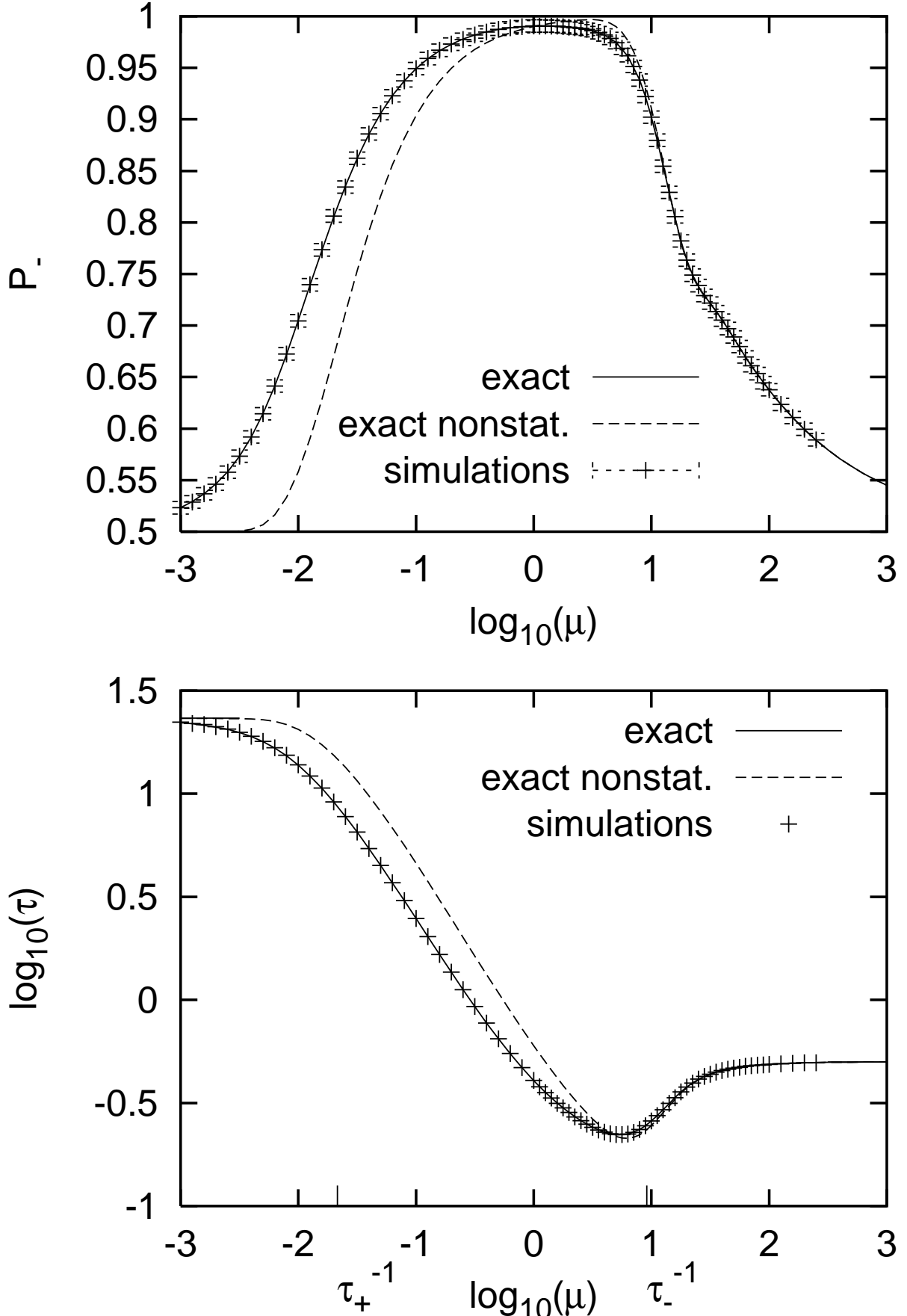


FIG. 3: A detailed study of the deterministic switching case. ABCO and MFPT for the stationary deterministic switching (solid line) and non-stationary deterministic switching (dashed line) are supplemented by the results of Monte Carlo simulations (crosses) of the stationary case. For ABCO, the three standard deviations error bars are included. The τ_{\pm} denote the mean first passage times for the respective slopes of the potential. The limiting values of MFPT in the static limit (the average of both τ 's) and in the infinitely fast switching limit (motion in the average potential) are also shown by the bars.

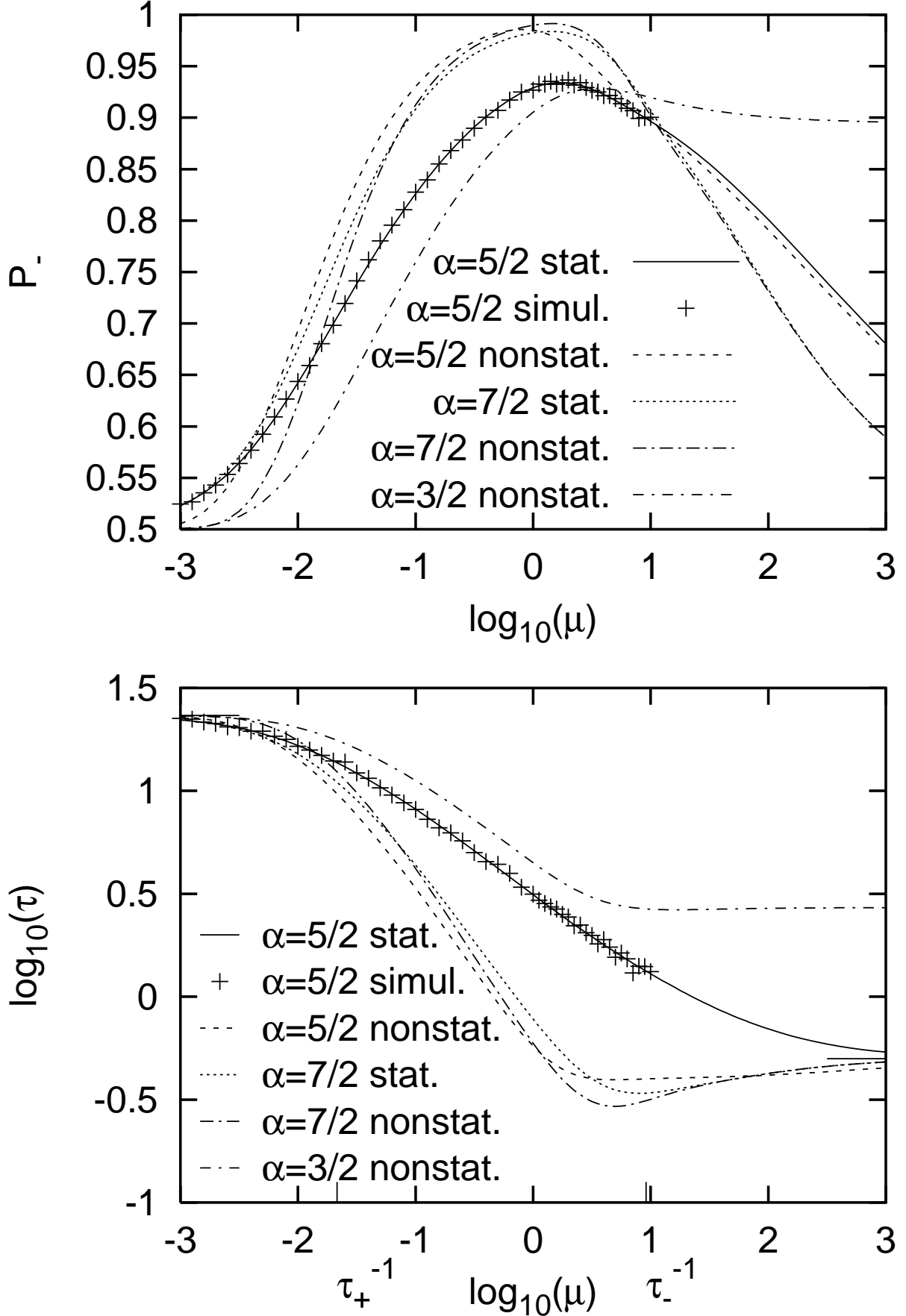


FIG. 4: ABCO for waiting time distributions without moments (power laws $t^{-\alpha}$ in asymptotics). The respective curves describes $\alpha = \frac{5}{2}$ stationary (solid line) and non-stationary (dashed line) cases, $\alpha = \frac{7}{2}$ stationary (dotted line) and non-stationary (long dash-dotted line) cases, and $\alpha = \frac{3}{2}$ non-stationary case (short dash-dotted line). The results of Monte Carlo simulations (without error bars) for $\alpha = \frac{5}{2}$ stationary case are also included. The τ_{\pm} denote the mean first passage times for the respective slopes of the potential. The limiting values of MFPT in the static limit (the average of both τ 's) and in the infinitely fast